# Quantum Chemical Study of Adsorption and Dissociation of $H_2S$ on the Gallium-Rich GaAs (001)-4 × 2 Surface

**Hong-Liang Lu, Wei Chen, Shi-Jin Ding, Min Xu, David Wei Zhang,* and Li-Kang Wang**

*State Key Laboratory of ASIC and System, Department of Microelectronics, Fudan University, Shanghai 200433, People's Republic of China*

*Received: December 13, 2005; In Final Form: March 27, 2006*

$H_2S$ adsorption and dissociation on the gallium-rich GaAs(001)-4 × 2 surface is investigated using hybrid density functional theory. Starting from chemisorbed $H_2S$ on the GaAs(001)-4 × 2 surface, two possible reaction routes have been proposed. We find that $H_2S$ adsorbs molecularly onto GaAs(001)-4 × 2 via the formation of a dative bond, and this process is exothermic with adsorption energy of 6.6 kcal/mol. For the first reaction route, one of the H atoms from the chemisorbed $H_2S$ is transferred to a second-layer As atom and the dissociated SH is inserted into the Ga−As bond with an activation barrier of 8.2 kcal/mol, which is found to be 29.3 kcal/mol more stable than the reactants. For the second case, the dissociated species may insert themselves into the Ga−Ga dimer resulting in the Ga−H−Ga and Ga−HS−Ga bridge-bonded states, which are found to be 29.8 and 22.2 kcal/mol more stable than the reactants, respectively. However, the calculations also show that the activation barrier (16.1 kcal/mol) for chemisorbed $H_2S$ dissociation through the second route is higher than the transfer of one H atom into a second-layer As atom. As a result, we conclude that sulfur insertion into the Ga−As bond is more kinetically favorable.

## 1. Introduction

III−V compound semiconductors such as gallium arsenide (GaAs) are among the most important semiconductor materials and are widely used in fast microelectronic devices due to their high carrier mobility, large-energy band gap, and low power consumption.[1−3] Although GaAs has desirable bulk properties, the application of this semiconductor in devices has been limited by its unwanted surface properties. A high defect density at the surface of GaAs-based devices, which has been thought to be related to the adsorption of impurities such as oxygen or water, detrimentally affects the electrical characteristics of the devices.[4,5] Therefore, it is essential to passivate the GaAs surface, especially with respect to atmospheric oxygen.

Many attempts have been reported to produce passivated GaAs surfaces with a reduced density of defect states through various methods. Formation of insulators on GaAs, such as molecular beam deposition of $Ga_2O_3(Gd_2O_3)$ or atomic layer deposition of $Al_2O_3$ and $HfO_2$, has been carried out recently.[6−10] However, high-quality insulator-GaAs interfaces remain difficult to achieve and studies of their electrical properties are still in progress. Surface treatment of a gallium arsenide semiconductor in sulfide-containing solutions has also attracted considerable attention in the past few years.[11,12] Great efforts have been devoted to constructing an effective passivation layer by using $Na_2S{\cdot}9H_2O$ and $(NH_4)_2S_x$ in wet chemical treatments. These treatments result in a dramatic decrease of the surface state density. Attendant reduction of the surface recombination velocity allows one to improve the performance and reliability of devices.[13−15] The resulting passivated surfaces, however, rapidly degraded in the ambient air, indicating that the layers created by wet chemical passivation are unstable in the presence of water and oxygen.[16] Such aqueous sulfur treatments are also prone to poor reproducibility and contamination with carbon and heavy metals.[17] Consequently dry passivation of GaAs in a vacuum, using $H_2S$ as the source of sulfur, has been proposed instead.[18,19] Unlike many wet chemical treatments for passivating GaAs surfaces, the use of a simple gas molecule ($H_2S$) is suitable for in situ deposition. In addition, the passivation layer formed by dry $H_2S$ shows a good resistance to oxidation and a high thermal stability.[20,21]

One of the first studies of $H_2S$ adsorption on GaAs surface was carried out by Massies et al. using auger electron spectroscopy (AES), low energy electron diffraction (LEED), and electron loss spectroscopy (ELS).[22] They suggested that the mechanism of $H_2S$ adsorption is temperature and coverage dependent. At room temperature and relatively low exposures, $H_2S$ adsorbs molecularly on GaAs (100) surface, while at higher temperature (700 K) the adsorbed $H_2S$ dissociate. Massies' view that the adsorption is mainly molecular at low temperature is not upheld by subsequent experimental works. Ranke et al. proposed that $H_2S$ adsorbed dissociatively to produce surface HS species preferentially bound to As on all orientations of GaAs at 150 K, while surface atomic sulfur was mainly bound to Ga with accompanied As depletion at 720 K.[23] At 720 K, surface sulfur also begins to penetrate into the lattice at high $H_2S$ exposures. Their results are also supported by Foord et al. who used high-resolution electron energy loss spectroscopy (HREELS), thermal desorption spectroscopy (TDS), and AES to investigate the adsorption of $H_2S$ on the Ga-rich GaAs (100)-4 × 1 surface.[24] They concluded that dissociation adsorption occurs initially to produce HS and H species at 190 K, with the latter bonded to both Ga and As. As the surface coverage of these species increases, molecular adsorption is also observed. It was found that more sulfur could be built up on the surface by repeated cycles of $H_2S$ exposure at low temperature with subsequent heating to 600 K.

More recently, Chuang and co-workers employed HREELS, LEED, and temperature programmed desorption (TPD) to investigate the surface chemistry of $H_2S$ on the GaAs (001)-4

* To whom correspondence should be addressed. Phone/Fax, +86 21 65642389; E-mail, dwzhang@fudan.edu.cn, dwzhang@fudan.ac.cn.

10.1021/jp057267a CCC: $33.50 © 2006 American Chemical Society
Published on Web 04/27/2006

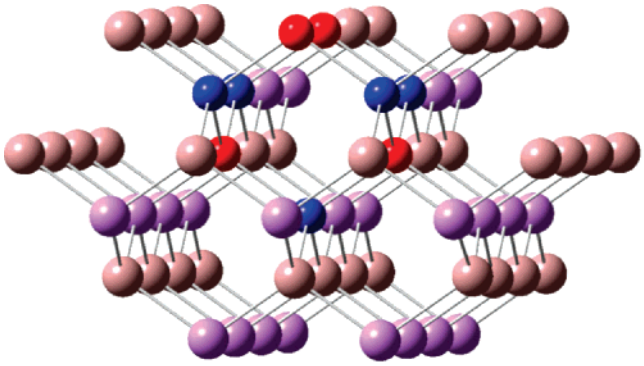

**Figure 1.** Perspective view of the GaAs (001) unreconstruction surface. The brown, purple, and white atoms represent Ga, As, and H atoms, respectively.

× 2 surface.[17,25−26] Their experimental evidence supported the fact that $H_2S$ initially adsorbs dissociatively to HS and H species on the GaAs (001)-4 × 2 surface with the hydrogen selectively bonded to As at 100 K. As a result, only the H−S and As−H stretching modes were monitored in their HREEL spectra, while the Ga−H stretching mode was not observed. On the other hand, the sulfur from HS dissociation is predominantly bonded to Ga after annealing to 700 K. Their results were confirmed by Wei et al. who found that the dissociative adsorption of $H_2S$ at 100 K produces only As−H species with a vibrational frequency of 2072 $cm^{-1}$.[27,28] Furthermore, the formation of Ga−H was also observed upon thermal annealing. Then they suggested that an energy barrier may exist between the two adsorption states of H atoms and the dissociative adsorption of $H_2S$ on the GaAs (100) surface involves an intermediate of Ga−HS−H−As. In addition, the bridging Ga−H−Ga species around 1460 $cm^{-1}$ were confirmed by Qi et al. in their IR spectroscopic studies.[29]

Despite these experimental works, little is reported about the adsorption, dissociation, and local geometry resulting from the interaction of $H_2S$ with the GaAs surface theoretically. To contribute to a better understanding of the molecule−surface interaction process, in the present work, the detailed chemical mechanism for the reaction of $H_2S$ at the gallium-rich GaAs-(001)-4 × 2 surface is studied using density functional theory (DFT) calculations. We performed geometry optimizations and calculated the energies of the stationary points on the potential energy surface (PES). Possible dissociation routes and their associated chemistry were investigated.

## 2. Calculation Methods

Ball-and-stick cluster models of the gallium-rich GaAs(001)-4 × 2 unreconstruction surface are shown in Figure 1. A molecular cluster, having the minimum size required to simulate this surface structure, is highlighted with red and blue spheres. This cluster contains two surface layers of Ga atoms representing the dimer structure, the four second-layer As atoms directly bonded to the dimer atoms, two-third-layer Ga atoms, and one-fourth-layer As atom. The "bulk" arsenic and gallium atoms are terminated by hydrogen atoms to avoid spin and charge contamination from the dangling bonds. And the number of H atoms is chosen so that the number of nonbonding electrons equals twice the number of 3-fold coordinated As atoms.[30,31] The $Ga_4As_5H_9$ single dimer cluster is then used to model the gallium-rich GaAs(001)-4 × 2 surface. In addition, to justify the validity of the cluster models used for GaAs, $Ga_7As_8H_{11}$ double-dimer cluster was also used to study the convergence of the results with cluster size. These two clusters are shown in parts a and b of Figure 2, respectively.

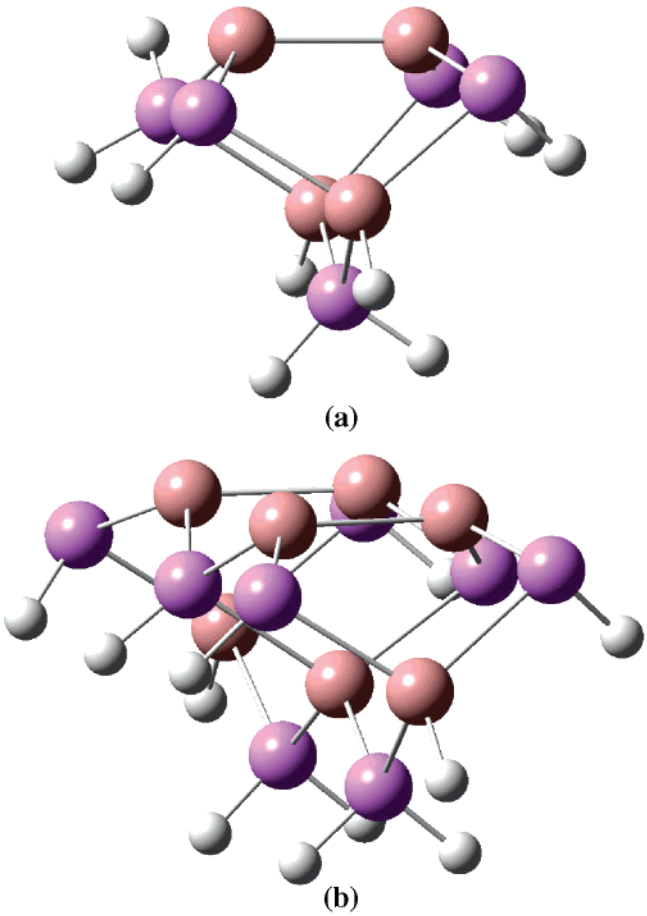


**Figure 2.** GaAs* surface modeled by (a) $Ga_4As_5H_9$ single-dimer cluster and (b) $Ga_7As_8H_{11}$ double-dimer cluster in the calculations. The brown, purple, and white atoms represent Ga, As, and H atoms, respectively.

In the present work, geometry optimizations and energy and frequency calculations are performed within the framework of DFT using the Gaussian 03 suite of electronic structure programs.[32] The results described here are obtained using the B3-LYP hybrid density functional, which corresponds to Becke's three-parameter exchange functional (B3) along with the Lee−Yang−Parr gradient-corrected correlation functional (LYP).[33] The electronic wave function is expanded using a Gaussian basis set. The S and H atoms are described using the 6-311+g(d,p) basis set, and Ga and As atoms are described using the LANL2DZ basis set. The dissociation routes from reactants to products are constructed by connecting the transition states with the intermediates. The optimizations are performed without any geometric constraints or symmetry restrictions. Frequency calculations are carried out after geometry optimizations to verify whether a minimum or a first-order saddle point is reached. All energies reported here include zero-point energy corrections. All energy minima are confirmed to have no imaginary frequencies, while the transition state structures have one single imaginary frequency.

## 3. Results and Discussion

For the optimized gallium-rich GaAs(001)-4× 2 surface modeled by single-dimer cluster, it is characterized by a Ga−Ga dimer. The Ga−Ga bond length of 2.56 Å is in agreement with the values of 2.60 and 2.45 Å, which were calculated by Fu et al.[30] and Northrup et al.,[34] respectively. For the $H_2S$ molecule, we found the following structural parameters: the bond lengths $d$(H−S) = 1.34 Å, α(H−S−H) = 92°. These

**TABLE 1: Representative Bond Lengths for the Structures of $H_2S$-CS, $H_2S$-TS1, $H_2S$-DS1 and Reaction Energies at 0 K ($\Delta H_0$) for GaAs* + $H_2S$[a]**

| | Ga−S | H(1)−S | H(2)−S | As−H | $\Delta H_0$ (single dimer) | $\Delta H_0$ (double dimer) |
|---|---|---|---|---|---|---|
| $H_2S$-CS | 2.69 | 1.35 | 1.35 | 4.14 | −6.6 | −7.07 |
| $H_2S$-TS1 | 2.47 | 1.68 | 1.35 | 1.87 | 1.6 | 2.88 |
| $H_2S$-DS1 | 2.28 | 4.19 | 1.35 | 1.51 | −29.3 | −27.4 |

[a] All bond lengths are shown in Å, while energies are shown in kcal/mol.

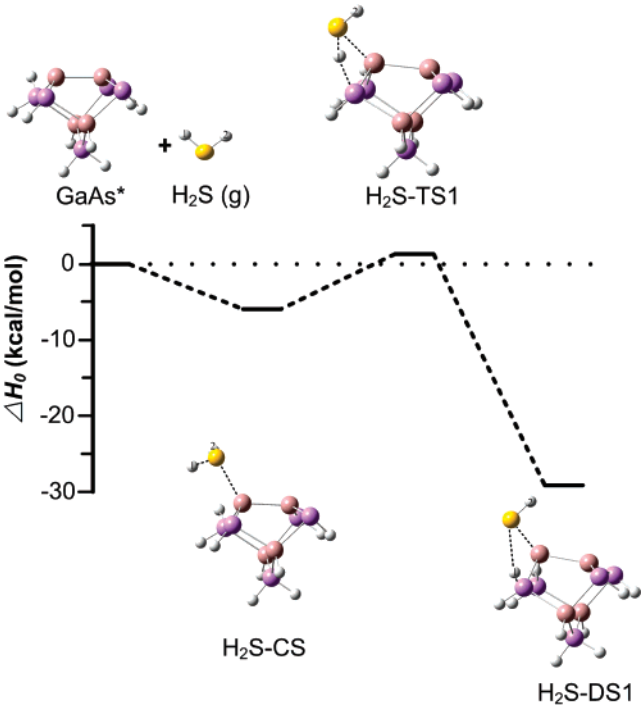


**Figure 3.** The first route and optimized geometries for the reaction of gaseous $H_2S$ on the GaAs* surface. $H_2S$-CS, $H_2S$-TS1, and $H_2S$-DS1 represent the $H_2S$ chemisorbed state, transition state, and dissociation state, respectively. The representative bonds are shown with dashed lines. The brown, purple, white, and yellow atoms represent Ga, As, H, and S atoms, respectively.

values are calculated to be 1.44 Å and 92° by Smardon et al.[35]

The surface reaction starts with the adsorption of $H_2S$ onto the GaAs surface to form a $H_2S$ chemisorbed state ($H_2S$-CS), in which $H_2S$ adopts a configuration adjacent to Ga−Ga dimer. The interaction between the sulfur lone-pair electrons and the empty Ga dangling bond results in the formation of a Ga−S dative bond. The optimized structural parameters for the $H_2S$-CS are listed in Table 1. The Ga−Ga dimer gets elongated by almost 0.8% for the chemisorbed state due to charge transfer between sulfur and gallium. And the H(1)−S bond length is found to increase from 1.34 Å in hydrogen sulfide molecules to 1.35 Å in $H_2S$-CS. The bond length between S and Ga atom is 2.69 Å, longer than the normal Ga−S bond of 2.37 Å.[36] It further confirms that the bond formed between Ga and S atoms is a dative bond. As can be seen from Figure 3, when $H_2S$ adsorbs molecularly on Ga−Ga dimer, the adsorption energy is 6.6 kcal/mol. So we can draw the conclusion that $H_2S$ adsorption on the GaAs(001)-4 × 2 surface is energetically favorable, having no activation energy.

To transform the dative bond into a covalent bond, one hydrogen atom must be released from the chemisorbed hydrogen sulfide molecule to a neighbor adsorption site. There are two possible dissociation routes through which this can occur: (1) transfer of one H atom from the chemisorbed $H_2S$ to a second-layer As atom; (2) insertion of the H atom into the Ga−Ga dimer and then transfer itself to the other Ga dangling bond.

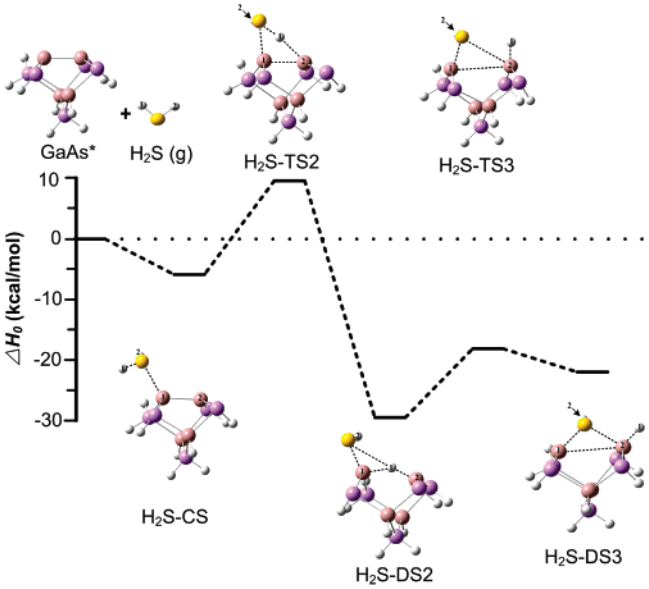


**Figure 4.** The second and third routes and optimized geometries for the reaction of $H_2S$ on the GaAs* surface. $H_2S$-CS, $H_2S$-TS2, $H_2S$-DS2, $H_2S$-TS3, and $H_2S$-DS3 represent the $H_2S$ chemisorbed state, the second transition state and dissociation state, and the third transition state and dissociation state, respectively. The representative bonds are shown with dashed lines. The brown, purple, white, and yellow atoms represent Ga, As, H, and S atoms, respectively.

The first route for chemisorbed $H_2S$ dissociation is the transfer of one H atom into a second-layer As atom, which is shown in Figure 3. The lengths of representative bonds shown with dashed lines in Figure 3, and the corresponding reaction energies are listed in Table 1. For the transition state ($H_2S$-TS1), only one imaginary frequency was found in the DFT calculation. A normal-mode analysis reveals that this imaginary frequency is associated with hydrogen transfer and that the trajectory of the H-atom movement is from $H_2S$ to the second layer As atom. As is expected, $H_2S$-TS1 has H(1)−S bond elongated by 0.22 Å compared to that in the $H_2S$-CS, consistent with the ultimate breaking of this bond. The Ga−S and As−H bond distances throughout the reaction go from 2.69 and 4.14 Å in the $H_2S$-CS to 2.47 and 1.87 Å in the transition state and finally contracting to 2.28 and 1.51 Å in the dissociation state ($H_2S$-DS1), respectively, indicating complete bond formation. From Figure 3 and the energies in Table 1, it can be seen that the energy barrier of 8.2 kcal/mol must be overcome to produce an HS species with respect to the $H_2S$-CS. This energy barrier indicates that a thermal activation would lead the system into the dissociative state. A higher-energy barrier indicates that corresponding reaction is kinetically more unfavorable. By consideration that the phenomenological approach in the form of the Arrehenius equation, with the choice for the attempt frequency ranging from $10^{13}$ and $10^{15}$ Hz, we have estimated that, for full dissociation, an activation barrier of 8.2 kcal/mol corresponds to a thermal activation in the range of 120−140 K.[37] This is in agreement with the experimental results that only As−H species are observed at 100−150 K. Finally, we observe that the dissociative state is 22.7 kcal/mol more stable than the $H_2S$-CS.

The second route for $H_2S$ on the GaAs(001)-4 × 2 surface is shown in Figure 4. Representative bond lengths are also shown in Table 2. In this case, one of the hydrogen atom detached from the $H_2S$ first inserts into the Ga−Ga dimer bond,

**TABLE 2: Representative Bond Lengths for the Structures of $H_2S$-TS2, $H_2S$-DS2, $H_2S$-TS3, $H_2S$-DS3 and Reaction Energies at 0 K ($\Delta H_0$) for GaAs* + $H_2S$**

| | Ga(1)−S | H(1)−S | H(2)−S | Ga(1)−H | Ga(2)−H | Ga(1)−Ga( 2) | $\Delta H_0$ (single dimer) | $\Delta H_0$ (double dimer) |
|---|---|---|---|---|---|---|---|---|
| $H_2S$-TS 2 | 2.51 | 1.67 | 1.35 | 1.84 | 2.26 | 2.69 | 9.5 | 9.8 |
| $H_2S$-DS 2 | 2.26 | 3.27 | 1.35 | 1.81 | 1.71 | 3.34 | −29.8 | −27.8 |
| $H_2S$-TS 3 | 2.24 | | 1.35 | | 1.57 | 4.13 | −18.1 | −19.6 |
| $H_2S$-DS 3 | 2.31 | | 1.35 | | | 3.87 | −22.2 | −24.1 |

[a] All bond lengths are shown in Å, while energies are shown in kcal/mol.

generating a bridging Ga−H−Ga bond. The transition state ($H_2S$-TS2) has Ga−S and H(1)−S bond lengths of 2.51 and 1.67 Å, which are shortened by 7% and elongated by 24% compared with the structural parameters of the $H_2S$-CS, respectively. A high activation barrier of 16.1 kcal/mol is needed for the dissociation reaction of H insertion into the Ga−Ga dimer with respect to the energy of the $H_2S$-CS. The Ga−S bond length in the dissociation state ($H_2S$-DS2) is 2.26 Å, which is 0.25 Å less than corresponding distances in the $H_2S$-TS2. It is obvious that the overall reaction is exothermic by 29.8 kcal/mol relative to the reactants, suggesting that this dissociation is thermodynamically favorable.

After H inserts into the Ga−Ga dimer, it may transfer itself to Ga(2) atom, forming a bridge-bonded HS species between and Ga(1) and Ga(2) atoms, as shown in Figure 4. This dissociation reaction also has an activation barrier of 11.7 kcal/mol to be overcome. The bond lengths for Ga(1)−S, Ga(2)−S, and Ga(2)−H are 2.31, 2.73, and 1.57 Å in the dissociation state ($H_2S$-DS3), respectively. The energy of the dissociated Ga−SH and Ga−H species is 22.2 kcal/mol relative to the separated reactants. It can be predicted that the formation of Ga−SH and Ga−H species is endothermic by 7.6 kcal/mol relative to the $H_2S$-DS2.

We have also made investigations on the mechanism involving the migration of an H-atom from a second-layer As atom to surface Ga atoms. However, the transition state connecting $H_2S$-DS1 and $H_2S$-DS2 is 38 kcal/mol higher in energy than $H_2S$-DS1. It is obvious that the reaction has the largest activation barrier of the reactions considered here. As a result, this reaction is quite unlikely.

Larger cluster can be employed to check for numerical convergence of calculation results.[38] In the present work, a double surface Ga dimers cluster shown in Figure 2b was used to calculate the reaction energies along the reaction routes mentioned above in a similar way. The calculated energies are also listed in Tables 1 and 2. It can be seen that the results obtained using the double-dimer cluster are in close agreement to those calculated using the single-dimer cluster, with energy difference of less than 2 kcal/mol. Therefore, the single-dimer cluster used throughout this study is a good model of the surface active sites since it is sufficient to describe the surface reactions.

From the results mentioned above, it can be seen that the lowest activation barrier for the overall reaction is the route that inserts the H atom into the Ga−As back bond. More importantly, the calculated activation energies for hydrogen insertion into the Ga−Ga dimer and H transfer to another Ga atom are both relatively high. Therefore, we predict that the formation of the Ga−H−Ga and Ga−H species is kinetically unfavorable, and high temperatures are required for this reaction. These results are consistent with the corresponding experiments.

## 4. Conclusions

In conclusion, we have investigated the initial reaction mechanism of $H_2S$ on the gallium-rich GaAs(001)-4 × 2 surface using DFT calculations. The reaction routes and representative bond lengths for three possible reaction routes are presented. The adsorption process is barrierless and the adsorption energy is 6.6 kcal/mol. Our calculation results show that transfer of one H atom from the chemisorbed $H_2S$ to a second-layer As atom, with an activation barrier of 8.2 kcal/mol, is more kinetically favorable than insertion of an H atom into the Ga dimer bond or transfer of one H atom to the other Ga dangling bonds, which is in very good agreement with the experimental values.

**Acknowledgment.** This work is supported by Science and Technology Committee of Shanghai under Grant No. 04JC14013, the Program for New Century Excellent Talents in University (NCET -04-0366), and the Shanghai Pujiang Program (05PJ-14017).

## References and Notes

(1) Hong, M.; Kwo, J.; Kortan, A. R.; Mannaerts, J. P.; Sergent, A. M. *Science* **1999**, *283*, 1897.
(2) Mimura, T.; Fukuta, M. *IEEE Trans. Electron Dev.* **1980**, *ED-27*, 1147.
(3) Chen, E. I.; Holonyak, N., Jr.; Maranowski, S. A. *Appl. Phys. Lett.* **1995**, *66*, 2688.
(4) Spicer, W. E.; Liliental-Weber, Z.; Weber, E.; Newmann, N.; Kendelewicz, T.; Cao, R.; McCants, C.; Mahowald, P.; Miyano, K.; Lindau, I. *J. Vac. Sci. Technol. B* **1988**, *6*, 1245.
(5) Kang, M. G.; Park, H. H. *Vacuum* **2002**, *67*, 91.
(6) Passlack, M.; Hong, M.; Mannaerts, J. P. *Appl. Phys. Lett.* **1996**, *68*, 1099.
(7) Passlack, M.; Medendorp, N.; Zollner, S.; Gregory, R.; Braddock, D. *Appl. Phys. Lett.* **2004**, *84*, 2521.
(8) Ye, P. D.; Wilk, G. D.; Kwo, J.; Yang, B.; Gossmann, H.-J. L.; Frei, M.; Chu, S. N. G.; Mannaerts, J. P.; Sergent, M.; Hong, M.; Ng, K. K.; Bude, J. *IEEE Electron Dev. Lett.* **2003**, *24*, 209.
(9) Frank, M. M.; Wilk, G. D.; Starodub, D.; Gustafsson, T.; Garfunkel, E.; Chabal, Y. J.; Grazul, J.; Muller, D. A. *Appl. Phys. Lett.* **2005**, *86*, 152904.
(10) Fanciulli, M.; Spiga, S.; Scarel, G.; Tallarida, G.; Wiemer, C.; Seguini, G. *Mater. Res. Soc. Symp. Proc.* **2004**, *E6.14.1*.
(11) Zeisse, C. R.; Messick, L. J.; Lile, D. L. *J. Vac. Sci. Technol.* **1977**, *14*, 957.
(12) Yang, J. K.; Kang, M. G.; Park, H. H. *J. Appl. Phys.* **2004**, *96*, 4811.
(13) Yablonovitch, E.; Sandroff, C. J.; Bhat, R.; Gmitter, T. *Appl. Phys. Lett.* **1987**, *51*, 439.
(14) Lu, Z. H.; Landheer, D.; Baribeau, J.-M.; Huang, L. J.; Lau, W. W. *Appl. Phys. Lett.* **1994**, *64*, 1702.
(15) Dong, Y.; Ding, X, M.; Hou, X. Y.; Li, Y.; Li, X. B. *Appl. Phys. Lett.* **2000**, *77*, 3839.
(16) Sandroff, C. J.; Hedge, M. S.; Chang, C. C. *J. Vac. Sci. Technol. B* **1989**, *7*, 841.
(17) Chung, C.-H.; Yi, S. I.; Weinberg, W. H. *Appl. Phys. Lett.* **1996**, *69*, 3369.
(18) Tiedje, T.; Colbow, K. M.; Rogers, D.; Fu, Z.; Eberhardt, W. *J. Vac. Sci. Technol. B* **1989**, *7*, 837.
(19) Kawanishi, H.; Sugimoto, Y.; Akita, K. *J. Vac. Sci. Technol.* **1991**, *9*, 1535.
(20) Kawanishi H.; Sugimoto, Y.; Akita, K. *J. Appl. Phys.* **1991**, *70*, 805.
(21) Wang, X. S.; Weinberg, W. H. *J. Appl. Phys.* **1994**, *75*, 2715.
(22) Massies, J.; Dezaly, F.; Linh, N. T. *J. Vac. Sci. Technol*. **1980**, *17*, 1134.
(23) Ranke, W.; Drathen, P.; Jacobi, K. *Surf. Sci.* **1978**, *77*, L162.
(24) Foord, J. S.; TitzGerald, E. T. *Surf. Sci.* **1994**, *306*, 29.
(25) Chung, C.-H.; Yi, S. I.; Weinberg, W. H. *J. Vac. Sci. Technol. A* **1997**, *15*, 1163.

(26) Yi, S. I.; Chung, C.-H.; Weinberg, W. H. *J. Vac. Sci. Technol. A* **1997**, *15*, 1168.
(27) Wei, X. M.; Liu, Q. P.; Zou, Z.; Xu, G. Q. *Appl. Phys. Lett.* **1998**, *73*, 2793.
(28) Zou, Z.; Wei, X. M.; Liu, Q. P.; Huang, H. H.; Sim, W. S.; Xu, G. Q.; Huan, C. H. A. *Chem. Phys. Lett.* **1999**, *312*, 149.
(29) Qi, H.; Gee, P. E.; Hicks, R. F. *Phys. Rev. Lett.* **1994**, *72*, 250.
(30) Fu, Q.; Li, L.; Li, C. H.; Begarney, M. J.; Law, D. C.; Hicks, R. F. *J. Phys. Chem. B* **2000**, *104*, 5595.
(31) Fu, Q.; Li, L.; Hicks, R. F. *Phys. Rev. B* **2000**, *61*, 11034.
(32) Frisch, M. J., et al. *Gaussian 03*, revision B.05; Gaussian: Pittsburgh, PA, 2003.
(33) Becke, A. D. *J. Chem. Phys.* **1993**, *98*, 1372.
(34) Northrup, J. E.; Froyen, S. *Mater. Sci. Eng. B* **1995**, *30*, 81.
(35) Smardon, R. D.; Srivastava, G. P. *Surf. Sci.* **2005**, *584*, 161.
(36) Kohler, T.; Frauenheim, T.; Hajnal, Z.; Seifert, G. *Phys. Rev. B* **2004**, *69*, 193403.
(37) Pilling, M. J.; Seaking, P. W. *Reaction Kinetics*; Oxford Science: Oxford, 1995.
(38) Widjaja, Y.; Musgrave, C. B. *J. Chem. Phys.* **2002**, *117*, 1931.